Assessing the Readiness of Numerical Relativity for LISA and 3G Detectors

Deborah Ferguson[1], Karan Jani[2], Pablo Laguna[1], and Deirdre Shoemaker[1]

[1] *Center for Relativistic Astrophysics and School of Physics, Georgia Institute of Technology, Atlanta, GA 30332*

[2] *Department of Physics and Astronomy, Vanderbilt University, Nashville, TN 37235*

Future detectors such as LISA promise signals at signal-to-noise ratios potentially in the thousands and data containing simultaneous signals. Is numerical relativity prepared for this new data analysis challenge? We estimate the minimum resolution a simulation must have as a function of signal-to-noise ratio in order to be indistinguishable from a true binary black hole signal of the same parameters. We demonstrate how numerical errors may leave residuals that could obscure higher modes and elaborate on the fractional loss of signal-to-noise ratio by using numerical templates.

Introduction: The Laser Interferometer Gravitational-wave Observatory (LIGO) and Virgo [1, 2] have ushered in the field of gravitational wave (GW) astronomy, a field that will enter a new era as the sensitivity of GW observatories improve and access new GW frequency bands [3, 4]. Together with experiment and data analysis, theory has been a partner in the success of the GW enterprise; it will, therefore, need to match the increase in sensitivity and reach of the detectors. In particular, numerical relativity (NR) has played a crucial role in the detection and interpretation of GWs from merging black holes (BHs) and neutron stars. The waveforms extracted from NR simulations have been used both to construct models [5–9] in direct analysis of the data [10], and as injections to stress test the detection pipeline[11]. It is crucial that NR codes have the capability to create waveforms at standards that will allow the community to capitalize on the wealth of information that will be provided by future detectors. If the source modeling is not on par with the advances on the experimental front, the data analysis that goes into detecting and characterizing signals will be seriously compromised.

Differences between a template waveform and a gravitational wave signal could have many origins, including but not limited to, using the "wrong" theory of gravity, using an approximate theory of gravity, or having differences in the parameters of the system. Such errors or missing physics in the template waveform have the potential to lead to misleading or incorrect results. Assuming general relativity (GR) is the correct gravitational theory, the solutions to the vacuum Einstein equations, as well as the waveforms extracted from the solutions, only have errors associated with numerical discretization. This is in contrast with simulations containing neutron stars where the micro-physics of the stars is not well understood nor is the impact on the waveforms. We will focus only on waveforms generated by evolving binary black holes (BBHs) in vacuum under Einstein's theory of GR. Fig. 1 shows an example of how the use of a low resolution template, one with significant discretization errors, can lead to residuals remaining in the data after the template is used to match the signal. We show this in comparison

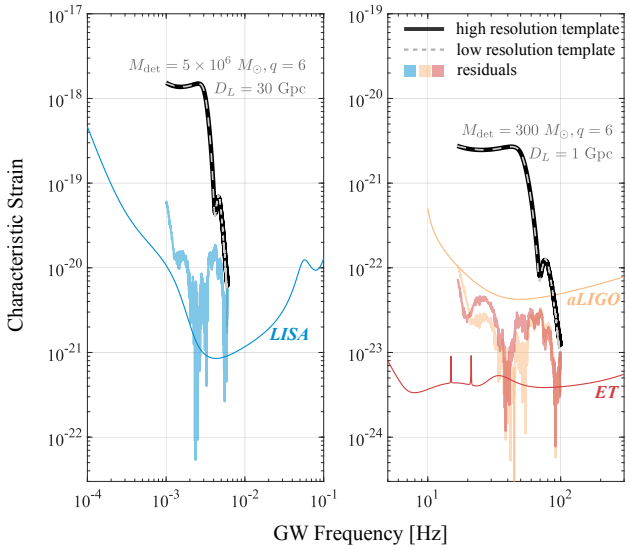

FIG. 1: Strains (gray) for $q = 6$ sources with an aligned spin of $a = 0.2$ on the larger BH; also plotted are noise curves and the residuals remaining in the data after using a low resolution template to match the signal (high resolution waveform).

to the noise curves of the Laser Interferometer Space Antenna (LISA) [12], the Einstein Telescope (ET) [4], and Advanced LIGO at design sensitivity [13, 14]. This is for an unequal mass binary of mass ratio 6:1 with a small spin of 20% maximal on the larger BH.

To further stress the importance of having high resolution in unequal mass ratio binaries for which higher modes are relevant, we show in Fig. 2 the strain of the same binary but now at an inclination of $\iota = 15^0$ for LISA, along with two residuals [3, 15]. The blue dashed line is a low resolution waveform and the solid blue line is the residual resulting from using that waveform as the template in matched filtering. The red dashed line is a high resolution waveform containing only the $(l, m) = (2, 2)$ mode, with the solid red line showing the residual resulting from using it as the template waveform. Notice that the two residuals are comparable, both

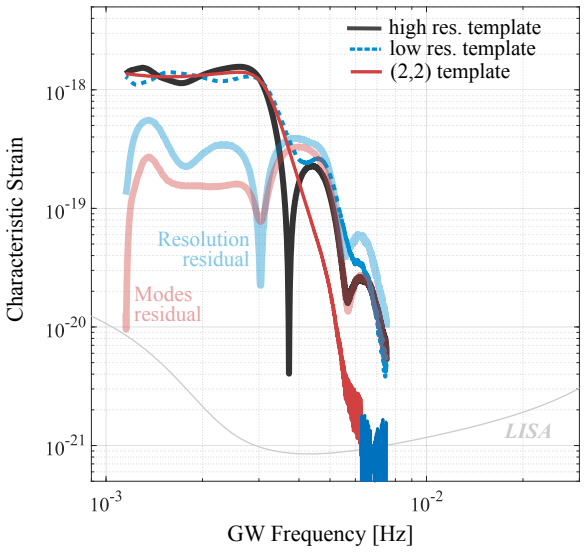

FIG. 2: Strain (black line) of a high resolution $(q, \iota) = (6, 15^o)$ source with an aligned spin of $a = 0.2$ on the larger BH for LISA at a distance of 30 Gpc, $\rho = 976$. The blue dashed line is a low resolution waveform of the same source parameters, with the solid blue line denoting the residual resulting from using it as the template. The red dashed line is a high resolution template containing only the $(l, m) = (2, 2)$ mode, with the solid red line showing the residual resulting from using it as the template waveform.

in strength and even in structure for this case, although we note that the structure of the residual will change depending on the details of the match and waveform.

Several studies have explored the potential impact that numerical errors could have on interpreting LIGO data [11, 16–18], including bounds on the numerical errors necessary for detection as well as for measurement [16, 19, 20]. Ref. [17] presents follow up work detailing different methods of assessing the accuracy of waveforms and the appropriate scenarios for each measure. Ref. [21] discusses the requirements on waveform model accuracy in order to be prepared for third-generation ground-based detectors and the relative errors in NR waveforms. While NR simulations produce waveforms for which the numerical errors are less significant than the noise associated with the current detectors, this will likely change as the sensitivity of the detectors increases.

The focus of this work is to investigate the impact of the errors associated with NR simulations of BBHs. We present a metric to access the errors arising from using a discrete resolution in NR waveforms and use that metric to estimate the minimum resolution required of NR simulations to produce waveforms indistinguishable from the true signal as a function of signal-to-noise ratio (SNR) in the context of LIGO, LISA, and ET [4, 22]. We also demonstrate how using templates with low resolution may leave residuals that could potentially obscure or be confused with higher order modes.

NR Waveforms: Our results are based on the Maya (formerly known as Georgia Tech) catalog of waveforms [23] produced using the `MAYA` code [24–27], a branch of the `Einstein Toolkit` [28] which is a NR finite-differencing code that evolves the BSSN formulation [29, 30] built upon `Cactus`, with mesh refinement from `Carpet` [31]. The simulations used in this study were performed on a grid with 10 refinement levels with the largest grid radii being $409.6\,M$ and the smallest grid radii being $0.2\,M$ $(0.1\,M)$ for mass ratios of 1:1 (6:1). The inspiral parameters quoted for this study are computed at the beginning of the simulation, but there is evidence that the excess radiation emitted at the beginning of an NR simulation does not significantly impact the values of the parameters [32].

As with all BSSN codes, our `MAYA` code computes waveforms from the Weyl Scalar Ψ_4 extracted at a finite radius away from the BBH and then extrapolated to infinity [33]. In order to avoid introducing additional errors from the extrapolation procedure, for this study, all waveforms have been extracted at a radius $75\,M$. We have checked that our results do not change significantly when using other extraction radii. The strain, h, is given by the second time integral of Ψ_4. To facilitate analysis, the strain is decomposed in terms of spin-weighted spherical harmonics ${}_{-2}Y_{l,m}$, of which the $(l, m) = (2, 2)$ quadrupole mode is generally the most dominant. In the present work, we only use the modes: $(2, 1), (2, 2), (3, 2), (3, 3), (4, 3)$ and $(4, 4)$.

For the binary masses detected and expected, NR simulations are not generally able to produce waveforms with enough cycles to cover the sensitive frequency range of the LIGO and Virgo detectors. This will be even more significant for LISA and ET. To circumvent this, NR waveforms are stitched to approximates (e.g. post-Newtonian), thus creating hybridized waveforms [34]. However, since the goal of this paper is to analyze specifically the truncation error associated with limited NR resolution, we are using only the NR waveform and computing the relevant quantities over the frequency range spanned by it. The starting frequencies for a total mass of $1M_\odot$ are provided by the NR waveforms, and we divide by total mass to obtain the desired frequency. For the NR waveforms utilized in this study, this means a total mass of $1\,M_\odot$ would have a starting frequency $f_{lower} = 2043$ Hz for the equal mass scenario and $f_{lower} = 4772$ Hz for the case with mass ratio 6:1. These should be scaled according to the total mass in each case.

Metric for Accessing Accuracy: A waveform h_i extracted from a NR simulation will differ from the exact solution h by an error δh_i; that is, $h_i = h + \delta h_i$. Since our code uses

finite differencing, to leading order we have $\delta h_i = c\,\Delta_i^\alpha$. Here α is the convergence rate of the code, c depends on derivatives of h, and Δ_i is the characteristic discretization scale, or grid-spacing, used in the simulation. Due to our use of adaptive mesh refinements, Δ_i will refer to the grid spacing of our finest mesh, which covers the smallest of the two initial BHs.

By carrying out simulations of different resolutions, one can determine the convergence rate α of the code and extrapolate h_i to infinite resolution and, in principle, obtain h in a process called Richardson extrapolation [35]. Computing matches between a finite resolution template and the Richardson extrapolated waveform would be an ideal way to quantify the errors associated with limited resolution. However, effects from boundary refinements [31], extrapolations during temporal stepping, and outer boundary conditions, to name a few, make the process of Richardson extrapolation more challenging. Therefore, to approximate the truncation errors of a given resolution, we compute the relative errors between multiple simulations of different resolutions and, by doing this for multiple pairs of resolutions, compute our code's convergence rate and express the impact of the truncation errors as a function of resolution. To compute α we make use of a $q = 1$ BBH system with aligned, dimensionless spin of $a = 0.6$ for which we have multiple resolutions. By keeping the higher resolution waveform fixed at $\Delta_1 = 200$ and varying the lower resolution template, we compute $\alpha = 4$. As our simulations are performed using $6th$ order spatial finite-differencing and $4th$ order Runge-Kutta for time evolution, this value of convergence rate is consistent.

With the convergence rate established, let us consider the overlap of two NR waveforms, h_1 and h_2:

$$\mathcal{O}[h_1, h_2] \equiv \frac{\langle h_1|h_2\rangle}{\sqrt{\langle h_1|h_1\rangle\langle h_2|h_2\rangle}}, \tag{1}$$

where

$$\langle h_1|h_2\rangle = 2\int_0^\infty \frac{h_1^* h_2 + h_1\, h_2^*}{S_n} df\,, \tag{2}$$

with S_n being the one-sided power spectral density of the detector, and $*$ denoting the complex conjugate. Expanding Eq. 1 to second order in the truncation error [36]:

$$\mathcal{O}[h_1, h_2] \approx 1 - \frac{1}{2}\left(\Delta_2^\alpha - \Delta_1^\alpha\right)^2 \frac{\langle c|c\rangle}{\langle h|h\rangle}\left[1 - \mathcal{O}^2[h, c]\right]. \tag{3}$$

Noting that c depends on derivatives of h, we can approximate that $\mathcal{O}^2[h, c] \approx 0$ and write Eq. 3 in terms of the mismatch, $\epsilon = 1 - \max_{t_0\phi_0} \mathcal{O}$, as

$$\epsilon[h_1, h_2] = \frac{\beta^2}{2}\left(\Delta_2^\alpha - \Delta_1^\alpha\right)^2, \tag{4}$$

with $\beta^2 = \langle c|c\rangle/\langle h|h\rangle = \langle c|c\rangle/\rho^2$ and $\rho = \langle h|h\rangle^{1/2}$ being the SNR.

Following [16], a NR waveform will be indistinguishable by the detector from the true signal if and only if: $\langle \delta h|\delta h\rangle < 1$, or equivalently $\Delta^{2\alpha}\langle c|c\rangle < 1$. We propose a new version of this metric for accessing accuracy written in terms of β as

$$\rho < \frac{1}{\beta\,\Delta^\alpha}, \tag{5}$$

allowing a *direct* computation between SNR and NR discretization.

Applying Accuracy Metric to Detectors: Once we obtain values for α and β, Eq. 5 provides the SNRs for which a NR waveform of a given resolution will be indistinguishable from a signal of the same parameters. Using simulations with multiple different resolutions, we compute mismatches ϵ to obtain α and β from Eq. 4. It is important to keep in mind that β depends on both the detector and the parameters of the source (mass M_{det}, mass ratio q, spins a, and inclination ι). Here we define mass ratio such that $q \geq 1$. For this analysis, we primarily consider total masses in the detector frame of $M_{det} = 300M_\odot$ for ET and LIGO and $M_{det} = 5 \times 10^6 M_\odot$ for LISA.

We explore the values of β for three different BBH systems each for LIGO, ET, and LISA. For the equal mass BBH case, we keep the higher resolution waveform fixed at $\Delta_1 = M/200$ and consider lower resolutions of $\Delta_2 = M/80$, $M/120$, and $M/140$. Using these, we compute $\beta \approx 10^6$ for all three detectors. For unequal mass simulations, finer resolution is required to fully resolve the smaller initial black hole. Therefore, for a $q = 6$ BBH with the more massive BH having an aligned, dimensionless spin of $a = 0.2$, we use resolutions of $\Delta_1 = M/280$ and $\Delta_2 = M/200$ to obtain $\beta \approx 10^7$ when observed with $\iota = 0$ and $\beta \approx 5 \times 10^8$ when observed with $\iota = 15^o$, in each of the detectors. While these values do change with total mass, they remain at the same order of magnitude.

Figure 3 shows Eq. 5 for $(q, \iota) = (1, 0^o)$ in the case of LIGO for several M_{det}. The horizontal line shows $\rho = 32.4$, the highest SNR yet observed by LIGO. The BBH case in this figure is characteristic of most of the $q \approx 1$ BBH systems observed so far. Since the NR waveforms used in the data analysis of those signals had resolutions $\Delta < M/120$, they were not distinguishable by LIGO from the true signal.

Looking towards the future detectors as well, Eq. 5 is plotted in Fig. 4 for all three detectors, LIGO, ET, and LISA. Each of the shaded regions show the values of ρ for which an NR waveform of a given resolution Δ is guaranteed to be indistinguishable from the true signal of the same parameters. Blue is for the case $(q, \iota) = (1, 0^o)$, and red is for the case $(q, \iota) = (6, 15^o)$. Below the red dashed line is the case $(q, \iota) = (6, 15^o)$. The vertical line shows the highest resolution Maya waveform in the LIGO

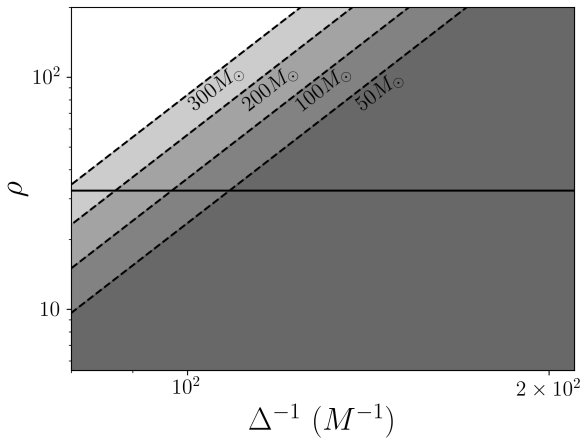

FIG. 3: Plot of $\rho < 1/(\beta\,\Delta^\alpha)$ where Δ is the resolution of a NR simulation for $(q, \iota) = (1, 0^o)$ with an aligned spin of $a = 0.6$ for both BHs in the case of LIGO for several M_{det}. The horizontal line shows $\rho = 32.4$, the highest SNR yet observed.

and Virgo Collaboration (LVC) catalog ($\Delta = M/400$). We do not include data below the lowest NR resolutions we analyze, $\Delta = M/80$ for $q = 1$ and $\Delta = M/200$ for $q = 6$.

For LISA and ET, it also appears that for low mass ratio cases, current NR waveforms will be sufficient at the expected SNRs. For the $(q, \iota) = (6, 0^o)$ case (red regions), NR waveforms at our current highest resolution ($\Delta = M/400$) would be sufficient for $\rho < 800$ for each of the detectors. Since it is expected that LISA and ET will be able to detect signals in the hundreds or thousands, it is clear from Fig. 4 that one would require resolutions of at least $\Delta \approx M/600$. The situation gets more challenging if the source has inclination, allowing higher modes to be more observable. For ET and LISA in the case $(q, \iota) = (6, 15^o)$, resolutions at the level of $\Delta \approx M/10^3$ are needed to reach $\rho \approx 10^3$.

Equation 5 also allows us to estimate the fractional loss of SNR due to numerical errors:

$$\frac{\delta\rho}{\rho} = \frac{\rho_i - \rho}{\rho} = \sqrt{\frac{\langle h_i|h_i\rangle}{\langle h|h\rangle}} - 1 \approx \frac{1}{2}\Delta^{2\alpha}\beta^2 < \frac{1}{2\,\rho^2}\,. \quad (6)$$

This equation allows us to see that for signals with large SNR, the fractional loss will be less than for low SNR signals.

Conclusions: Given the SNR of BBH signals, we have provided estimates of the resolution needed in NR finite-differencing codes to produce waveforms that are indistinguishable by the LIGO, LISA and ET detectors from the real signal, assuming that the template and the signal have the same parameters. We showed that for detections such as the ones obtained by LIGO so far, with $\rho < 40$, current finite-difference codes are capable of producing adequate waveforms if $\Delta < M/120$. We also showed that for high mass ratio binaries or binaries with inclination, where higher modes play an important role, NR codes need to improve significantly. To reach SNRs above a thousand, finite-difference NR code would have to efficiently scale to resolutions of at least $\Delta < M/700$. Being able to reach resolutions for template indistinguishability is particularly important because, as we demonstrated, residuals resulting from using lower resolution templates could be comparable to those resulting from ignoring higher modes entirely. While this paper investigates the relationship between resolution and SNR, there are alternative ways to increase the convergence rate of the codes, including increasing the finite-differencing order or implementing more efficient differencing schemes. The need for high quality NR waveforms may be alleviated if the very high SNR signals are not coincident in the detectors, allowing on-demand NR simulations to be deployed per high SNR event.

Our next step is to perform a parameter estimation study to understand how this NR truncation error translates to uncertainty in the physical parameters of the source. Furthermore, the present work was done using the methodology typical for LIGO data analysis, and simply using the noise curves for each detector. However, LISA's data analysis will be notably more complicated, and it will be a crucial future step to study the impact of these errors with LISA's data analysis machinery [37]. This is particularly important since it is expected that LISA will detect numerous signals concurrently.

Acknowledgements Work supported by NSF grants PHY-1806580, PHY-1809572, PHY-1550461 and 1333360. Computer resources provided by XSEDE TG-PHY120016, PACE at Georgia Tech, and LIGO supported by NSF grants PHY-0757058 and PHY-0823459. We thank Sascha Husa and Harald Pfeiffer for their insight.

[1] The LIGO Scientific Collaboration, Classical and Quantum Gravity **32**, 074001 (2015).
[2] F. Acernese et al. (VIRGO), Class. Quant. Grav. **32**, 024001 (2015), arXiv:1408.3978 [gr-qc].
[3] P. A. Seoane et al. (eLISA), (2013), arXiv:1305.5720 [astro-ph.CO].
[4] M. P. et al, Classical and Quantum Gravity **27**, 194002 (2010).
[5] M. Hannam, P. Schmidt, A. Boh, L. Haegel, S. Husa, F. Ohme, G. Pratten, and M. Prrer, Phys. Rev. Lett. **113**, 151101 (2014), arXiv:1308.3271 [gr-qc].
[6] A. Boh et al., Phys. Rev. D **95**, 044028 (2017), arXiv:1611.03703 [gr-qc].
[7] S. Khan, S. Husa, M. Hannam, F. Ohme, M. Prrer, X. Jimnez Forteza, and A. Boh, Phys. Rev. D **93**, 044007 (2016), arXiv:1508.07253 [gr-qc].

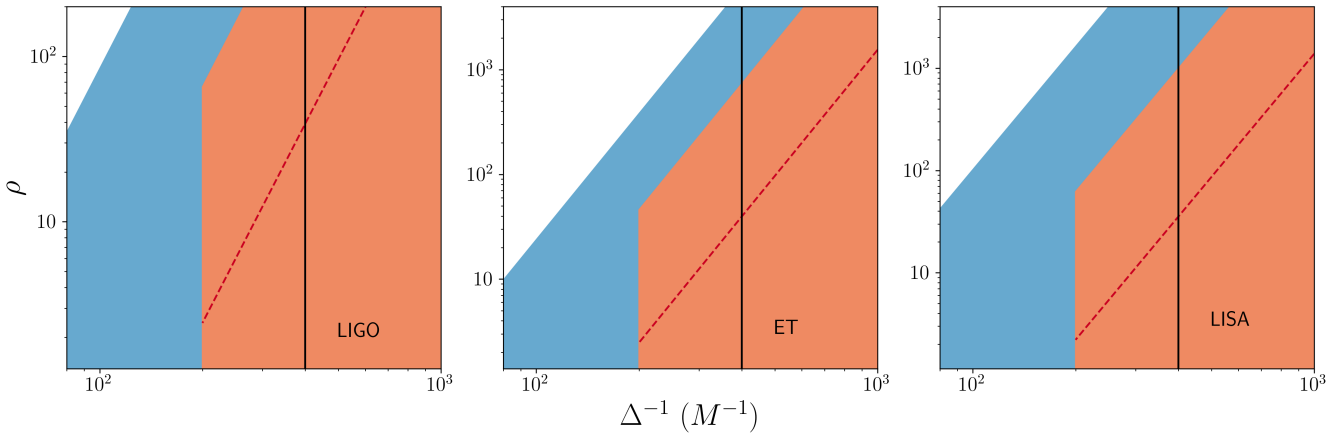

FIG. 4: Logarithmic plots of $\rho < 1/(\beta\,\Delta^{\alpha})$, where Δ is the resolution of a NR simulation. Blue shaded region is for $(q, \iota) = (1, 0^o)$ with $a = 0.6$ for both BHs and the red shaded region is for $(q, \iota) = (6, 15^o)$ with $a = 0.2$ for the larger BH. Overlapping with the red and below the dashed line is $(q, \iota) = (6, 15^o)$. The vertical line shows the highest resolution of our production runs ($\Delta = M/400$).

[8] J. Blackman, S. E. Field, M. A. Scheel, C. R. Galley, C. D. Ott, M. Boyle, L. E. Kidder, H. P. Pfeiffer, and B. Szilgyi, Phys. Rev. D **96**, 024058 (2017), arXiv:1705.07089 [gr-qc].

[9] S. Husa, S. Khan, M. Hannam, M. Prrer, F. Ohme, X. Jimnez Forteza, and A. Boh, Phys. Rev. D **93**, 044006 (2016), arXiv:1508.07250 [gr-qc].

[10] J. Lange et al., Phys. Rev. D **96**, 104041 (2017), arXiv:1705.09833 [gr-qc].

[11] P. Schmidt, I. W. Harry, and H. P. Pfeiffer, (2017), arXiv:1703.01076 [gr-qc].

[12] T. Robson, N. J. Cornish, and C. Liu, Classical and Quantum Gravity **36**, 105011 (2019).

[13] Abbott, B. P. et al. (KAGRA, LIGO Scientific, VIRGO), Living Rev. Rel. **21**, 3 (2018), arXiv:1304.0670 [gr-qc].

[14] LIGO Scientific Collaboration, "LIGO Algorithm Library - LALSuite," free software (GPL) (2018).

[15] P. Amaro-Seoane, H. Audley, S. Babak, J. Baker, E. Barausse, P. Bender, E. Berti, P. Binetruy, M. Born, D. Bortoluzzi, J. Camp, C. Caprini, V. Cardoso, M. Colpi, J. Conklin, N. Cornish, C. Cutler, K. Danzmann, R. Dolesi, L. Ferraioli, V. Ferroni, E. Fitzsimons, J. Gair, L. Gesa Bote, D. Giardini, F. Gibert, C. Grimani, H. Halloin, G. Heinzel, T. Hertog, M. Hewitson, K. Holley-Bockelmann, D. Hollington, M. Hueller, H. Inchauspe, P. Jetzer, N. Karnesis, C. Killow, A. Klein, B. Klipstein, N. Korsakova, S. L. Larson, J. Livas, I. Lloro, N. Man, D. Mance, J. Martino, I. Mateos, K. McKenzie, S. T. McWilliams, C. Miller, G. Mueller, G. Nardini, G. Nelemans, M. Nofrarias, A. Petiteau, P. Pivato, E. Plagnol, E. Porter, J. Reiche, D. Robertson, N. Robertson, E. Rossi, G. Russano, B. Schutz, A. Sesana, D. Shoemaker, J. Slutsky, C. F. Sopuerta, T. Sumner, N. Tamanini, I. Thorpe, M. Troebs, M. Vallisneri, A. Vecchio, D. Vetrugno, S. Vitale, M. Volonteri, G. Wanner, H. Ward, P. Wass, W. Weber, J. Ziemer, and P. Zweifel, arXiv e-prints , arXiv:1702.00786 (2017), arXiv:1702.00786 [astro-ph.IM].

[16] L. Lindblom, B. J. Owen, and D. A. Brown, Phys. Rev. **D78**, 124020 (2008), arXiv:0809.3844 [gr-qc].

[17] L. Lindblom, Phys. Rev. **D80**, 064019 (2009), arXiv:0907.0457 [gr-qc].

[18] I. Hinder et al., Class. Quant. Grav. **31**, 025012 (2014), arXiv:1307.5307 [gr-qc].

[19] E. E. Flanagan and S. A. Hughes, Phys. Rev. **D57**, 4566 (1998), arXiv:gr-qc/9710129 [gr-qc].

[20] M. Miller, Phys. Rev. D **71**, 104016 (2005).

[21] M. Pürrer and C.-J. Haster, Phys. Rev. Res. **2**, 023151 (2020), arXiv:1912.10055 [gr-qc].

[22] M. Abernathy et al., EGO (2011).

[23] K. Jani, J. Healy, J. A. Clark, L. London, P. Laguna, and D. Shoemaker, Class. Quant. Grav. **33**, 204001 (2016), arXiv:1605.03204 [gr-qc].

[24] F. Herrmann, I. Hinder, D. Shoemaker, and P. Laguna, Classical and Quantum Gravity **24**, S33 (2007), arXiv:gr-qc/0601026 [gr-qc].

[25] B. Vaishnav, I. Hinder, F. Herrmann, and D. Shoemaker, Phys. Rev. D **76**, 084020 (2007), arXiv:0705.3829 [gr-qc].

[26] J. Healy, J. Levin, and D. Shoemaker, Phys. Rev. Lett. **103**, 131101 (2009).

[27] L. Pekowsky, R. O'Shaughnessy, J. Healy, and D. Shoemaker, Phys. Rev. D **88**, 024040 (2013).

[28] F. Loffler et al., Class. Quant. Grav. **29**, 115001 (2012), arXiv:1111.3344 [gr-qc].

[29] T. W. Baumgarte and S. L. Shapiro, Phys. Rev. D **59**, 024007 (1999), arXiv:gr-qc/9810065.

[30] M. Shibata and T. Nakamura, Phys. Rev. D **52**, 5428 (1995).

[31] E. Schnetter, S. H. Hawley, and I. Hawke, Class. Quant. Grav. **21**, 1465 (2004), arXiv:gr-qc/0310042 [gr-qc].

[32] K. Higginbotham, B. Khamesra, J. P. McInerney, K. Jani, D. M. Shoemaker, and P. Laguna, Phys. Rev. D **100**, 081501 (2019).

[33] H. Nakano, J. Healy, C. O. Lousto, and Y. Zlochower, Phys. Rev. D **91**, 104022 (2015), arXiv:1503.00718 [gr-qc].

[34] P. Ajith et al., Class. Quant. Grav. **29**, 124001 (2012), [Erratum: Class.Quant.Grav. 30, 199401 (2013)], arXiv:1201.5319 [gr-qc].

[35] L. F. Richardson and R. T. Glazebrook, Proceedings of the Royal Society of London. Series A, Containing Papers of a Mathematical and Physical Character **83**, 335 (1910).

[36] B. Vaishnav, I. Hinder, F. Herrmann, and D. Shoemaker, Phys. Rev. D **76**, 084020 (2007), arXiv:0705.3829 [gr-qc].

[37] K. A. Arnaud et al., 6th International LISA Symposium, AIP Conf. Proc. **873**, 619 (2006), arXiv:gr-qc/0609105 [gr-qc].